Baseline-free absolute strain estimation for cylindrical structures

Ohjun Kwon [a], Hoon Sohn [a,*], Jinho Jang [a], Jaemook Choi [a], Zhanxiong Ma [a], Hyung Jin Lim [b]

[a] *Department of Civil and Environmental Engineering, KAIST, Daejeon 34141, Republic of Korea*
[b] *Department of Civil and Energy System Engineering, Kyonggi University, Suwon 16227, Republic of Korea*

ARTICLE INFO

ABSTRACT

The total strain induced by forces in a structure, known as absolute strain, provides crucial information about structural integrity. The unexpected variations in absolute strain can compromise the overall safety of the structural system. In this paper, a baseline-free absolute strain estimation technique is developed based on the acoustoelastic effect of ultrasonic guided wave for in-service cylindrical structures. To generate and sense ultrasonic guided waves, two macro-fiber composite (MFC) transducers were installed on the surfaces of cylindrical structures subjected to tensile force. Additionally, a strain gauge was used to measure the relative strain generated after installing the MFC transducers and the strain gauge. The absolute strain was estimated using the velocity of the ultrasonic guided waves and the relative strain, without the need for calibration tests and baseline data obtained from known absolute strain levels. The effectiveness of the developed technique was experimentally examined using blind data obtained from a hollow steel cylinder and an aluminum mooring cable from a submerged floating tunnel model.

1. Introduction

Cylindrical structures, such as hollow cylinders, mooring cables, rods, and PT tendons, are force-carrying members that play a critical role in maintaining the performance of structural systems [1,2]. Absolute strain, which refers to the total strain induced by forces in the current cylindrical structure, is an important structural engineering parameter for assessing the integrity and failure of a structural system [3]. Absolute strain changes mainly due to external impacts, natural disasters, and operating loads. Excessive increments of absolute strain in a cylindrical structure can result in performance deterioration and catastrophic failure of the structural system. Therefore, the estimation of absolute strain in cylindrical structures is essential to ensure the safety and performance of the structural system.

Several techniques have been developed to estimate absolute strain in cylindrical structures. Kerrouche et al. [4] installed a fiber Bragg grating (FBG) sensor on the surface of a carbon rod and correlated the reflected wavelength variation with absolute strain. FBG sensors have several advantages, such as immunity to electromagnetic noise, light weight, and long signal transmission distance. However, since FBG sensors require baseline data obtained before applying a force to estimate absolute strain, it is impossible to estimate absolute strain in-service cylindrical structures. Du and Gou [5] estimated the absolute

strain of a cable by comparing two images taken with a charge-coupled device camera (CCDC) before and after applying a force. However, the practical application of this technique is limited because it requires capturing an image before applying any force. Gulgec et al. developed a deep-learning-based absolute strain estimation method using acceleration data [6]. However, this method requires a calibration test to train the deep-learning model, where the input is the acceleration data, and the output is absolute strain. A passive wireless antenna sensor was developed to estimate absolute strain based on the shift in the electromagnetic resonance frequency of the antenna [7]. Strain gauges are mainly used to estimate absolute strain using the relationship between strain and electrical resistance [8]. However, antenna sensors and strain gauges without baseline data can only measure the relative strain generated additionally after installing the sensors when applied to the in-service cylindrical structures.

Ultrasonic techniques have been used to estimate absolute strain based on the acoustoelastic effect, which states that the velocity of ultrasonic guided waves has a linear relationship with the absolute strain within the elastic range. These techniques can achieve a long-distance wave propagation and high reliability, and the ultrasonic transducers are low cost, small size, and lightweight. Toyama and Takatsubo experimentally investigated the linear relationship between ultrasonic guided wave velocity and absolute strain in CFRP laminates under

---

tensile force [9]. Furthermore, this technique has been applied to stress estimation as well as absolute strain [10–12]. However, conventional ultrasonic techniques require calibration tests or baseline data to establish the relationship between the velocity of the ultrasonic guided waves and absolute strain or stress.

Conventional absolute strain estimation techniques for field applications require calibration tests or baseline data obtained from a known absolute strain levels. To address this limitation, in this study, a baseline-free technique was developed for estimating absolute strain of in-service cylindrical structures based on the acoustoelastic effect of ultrasonic guided wave. The linear relationship between the velocity of ultrasonic guided waves and absolute strain in cylindrical structures was derived and experimentally validated using a steel hollow cylinder. Two Macro Fiber Composites (MFC) transducers and one strain gauge are installed on the cylindrical structure subjected to tensile force to obtain the ultrasonic guided wave and the relative strain, respectively. The absolute strain was estimated from the ultrasonic guided wave and the relative strain measured after installing the sensors without the need for calibration tests and baseline data. The performance of the developed technique was evaluated using the steel hollow cylinder and an aluminum mooring cable from a submerged floating tunnel (SFT) model. The developed technique is unique in that (1) the linear relationship between the ultrasonic guided wave velocity and absolute strain is newly derived and experimentally verified, (2) the absolute strain is estimated without the need for calibration tests and baseline data, (3) the developed technique is experimentally validated in laboratory and ocean engineering basin, and (4) the developed technique is applicable to in-service cylindrical structures where the MFC transducers and the strain gauge are not initially installed before applying force.

This paper is organized as follows. Section 2 describes the derivation of the linear relationship between the ultrasonic guided wave velocity and absolute strain, as well as the procedure for estimating absolute strain without calibration tests and baseline data. Section 3 presents the validation of the derived linear relationship and the estimation of absolute strain in a steel hollow cylinder specimen under two different tensile force cases. Section 4, discusses the field applicability of the developed technique using the SFT model in an ocean engineering basin. Finally, a summary and conclusions are provided in Section 5.

2. Development of a baseline-free absolute strain estimation technique

2.1. Derivation of linear relationship between ultrasonic guided wave velocity and absolute strain

When an ultrasonic signal is applied to a cylindrical structure, cylindrical Lamb waves are generated and divided into longitudinal (L(0,β)), torsional (T(0,β)), and flexural (F(α, β)) modes based on wave propagation motion [13]. Here, α and β are the circumferential order and mode number, respectively (α = 1,2,3,…, β=1,2,3,…). Previous studies have reported that, among the three cylindrical Lamb wave modes, the L(0,1) velocity is the most sensitive to absolute strain variation and converges to the bar velocity when the frequency of the ultrasonic input signal approaches 0 kHz [14,15]. Therefore, the absolute strain estimation is performed using the L(0,1) mode. In addition, a low-frequency signal was used as the ultrasonic input signal in this paper, and it is assumed that the L(0,1) mode velocity is the same as the bar velocity. For instance, applying an ultrasonic input signal of 15 kHz to a hollow cylinder with an inner diameter of 5 mm, an outer diameter of 13 mm, an elastic modulus of 68.9 GPa, a density of 2.7 g/cm³, and a Poisson's ratio of 0.33 results in L(0,1) mode velocity of 5050 m/sec [16]. In addition, the bar velocity in the hollow cylinder is 5052 m/sec. The relative error between the two velocities is approximately 0.04%. This calculation suggests that the difference between the velocities of the bar and the L(0,1) mode can be neglected. The L(0,1) mode velocity is defined as [14]:

$$c = \sqrt{\frac{E}{\rho}} \tag{1}$$

where c is the L(0,1) mode velocity, E is the initial elastic modulus, and ρ is the initial density of the cylindrical structure in unperturbed state (i.e., without any applied force). When a tensile force is applied to the cylindrical structure in the x-direction, it induces absolute strain, which results in the variation of the elastic modulus and density, consequently altering the L(0,1) mode velocity.

First, the variation in the elastic modulus induced by absolute strain is investigated. The elastic modulus between two nonbonding atoms was described using the Lennard-Jones potential, which is given by the following equation [17,18]:

$$E_i^s = \epsilon \left[156 \frac{r_m^{12}}{r_i^{14}} - 84 \frac{r_m^6}{r_i^8} \right] \tag{2}$$

where E_i^s is the perturbed elastic modulus along the i-direction ($i = x, y, z$), ϵ is the depth of the potential well, r_m is the interatomic distance without any tensile force, and r_i is the perturbed interatomic distance along the i-direction when the tensile force is applied along the x-direction. When r_i is equal to r_m, the initial elastic modulus is $72\epsilon/r_m^2$. Dividing Equation (2) by the initial elastic modulus gives:

$$\frac{E_i^s}{E} = \frac{1}{72} \left[156 \frac{r_m^{14}}{r_i^{14}} - 84 \frac{r_m^8}{r_i^8} \right] \tag{3}$$

where r_m/r_i can be written as $1/(1+\varepsilon_i)$ [19], and ε_i is the absolute strain induced by the tensile force along the i-direction. By performing a Taylor expansion, the right-hand term in Equation (3) can be expressed as follows:

$$\frac{1}{72} \left[156 \frac{r_m^{14}}{r_i^{14}} - 84 \frac{r_m^8}{r_i^8} \right] = 1 - 21\varepsilon_i + 185.5\varepsilon_i^2 - 1073.3\varepsilon_i^3 + \cdots \tag{4}$$

By retaining the first and second terms of the right-hand term in Equation (4), Equation (3) can be approximated as:

$$\frac{E_i^s}{E} = 1 - 21\varepsilon_i \tag{5}$$

Next, the variation in density induced by the absolute strain is investigated. The initial density of the cylindrical structure is defined as follows:

$$\rho = \frac{m}{V} \tag{6}$$

where m and V are the initial mass and the initial volume of the cylindrical structure in the unperturbed state, respectively. m is constant even when the absolute strain occurs. The perturbed volume of the cylindrical structure can be expressed as:

$$V^s = l_x(1+\varepsilon_x)l_y(1+\varepsilon_y)l_z(1+\varepsilon_z) = V(1+\varepsilon_x)(1-\nu\mu\varepsilon_x)^2 \tag{7}$$

where V^s is the perturbed volume, ν is the Poisson's ratio, l_i is the initial length of the cylindrical structure along the i-direction, and ε_y and ε_z are computed as $-\nu\varepsilon_x$. The perturbed density is defined by substituting Equation (7) into Equation (6):

$$\rho^s = \frac{m}{V^s} = \frac{m}{V(1+\varepsilon_x)(1-\nu\varepsilon_x)^2} = \frac{\rho}{(1+\varepsilon_x)(1-\nu\varepsilon_x)^2} \tag{8}$$

Substituting Equations (5) and (8) into Equation (1) yields the following epression:

$$c_i^s = \sqrt{\frac{E_i^s}{\rho^s}} = c\sqrt{\frac{E_i^s \rho}{E\rho^s}} = c(1-\nu\varepsilon_x)\sqrt{(1+\varepsilon_x)(1-21\varepsilon_i)} \tag{9}$$

where c_i^s is the L(0,1) mode velocity propagating in the i-direction when

the absolute strain in the x-direction induced by the tensile force is ε_x. In this study, strain estimation was performed using c_x^s because it is the most sensitive to absolute strain among c_x^s, c_y^s, and c_z^s [1]. Based on Equation (9), c_x^s can be expressed as:

$$c_x^s = c(1 - \nu\varepsilon_x)\sqrt{(1 + \varepsilon_x)(1 - 21\varepsilon_x)} \tag{10}$$

By performing a Taylor expansion, the right-hand term in Equation (10) can be expressed as follows:

$$c(1 - \nu\varepsilon_x)\sqrt{(1 + \varepsilon_x)(1 - 21\varepsilon_x)} = c\left[1 - (\nu + 10)\varepsilon_x + (10\nu - 60.5)\varepsilon_x^2 + \cdots\right] \tag{11}$$

By retaining the first and second terms of Equation (11), Equation (10) can be approximated as:

$$c_x^s = c[1 - (\nu + 10)\varepsilon_x] \tag{12}$$

Equation (12) shows that c_x^s has a linear relationship with ε_x and decreases as ε_x increases.

2.2. Baseline-free absolute strain estimation

Fig. 1 shows a schematic of the sensor installation used to obtain the L(0,1) mode and relative strain. Two MFC transducers and one strain gauge were installed on the surface of the cylindrical structure at an unknown strain (ε_x^U) induced by an initial tensile force in the x-direction. The L (0,1) mode wave is generated by the excitation MFC, whereas its propagation in the x-direction is detected using the sensing MFC. The strain gauge is used to measure the relative strain (ε_x^R) generated in the x-direction after installing the sensors.

The procedure for the baseline-free absolute strain estimation is as follows. First, the L(0,1) mode is obtained after installing the sensors at ε_x^U. The L(0,1) mode velocity can be expressed as:

$$c_{xU}^s = c\left[1 - (\nu + 10)\varepsilon_x^U\right] \tag{13}$$

where c_{xU}^s is the measured L(0,1) mode velocity at ε_x^U. The L(0,1) mode velocity is computed using the following equation:

$$c_x^s = \frac{d_x}{t_x} \tag{14}$$

where d_x and t_x are the propagation distance and arrival time of the L (0,1) mode, respectively. The arrival time is measured using the peak-point method [20]. Subsequently, the L(0,1) mode is obtained when ε_x^R is induced by the variation in the tensile force after the MFC transducers and strain gauge have been already installed. The velocity of the additionally obtained L(0,1) mode can be expressed as:

$$c_{xR}^s = c\left[1 - (\nu + 10)\left(\varepsilon_x^U + \varepsilon_x^R\right)\right] \tag{15}$$

where c_{xR}^s is the L(0,1) mode velocity at $\varepsilon_x^U + \varepsilon_x^R$. Here, ε_x^R is obtained using the strain gauge. The velocity ratio of the L(0,1) mode measured at two absolute strain levels is given by:

$$\frac{c_{xR}^s}{c_{xU}^s} = \frac{1 - (\nu + 10)\left(\varepsilon_x^U + \varepsilon_x^R\right)}{1 - (\nu + 10)\varepsilon_x^U} \tag{16}$$

By rearranging Equation (16), ε_U is obtained as follows:

$$\varepsilon_x^U = \frac{1}{\nu + 10} + \frac{\varepsilon_x^R}{\frac{c_{xR}^s}{c_{xU}^s} - 1} \tag{17}$$

Finally, the absolute strain ε_x is estimated by adding ε_x^U, which is computed from Equation (17), and ε_x^R, which is measured with the strain gauge, as follows:

$$\varepsilon_x = \varepsilon_x^U + \varepsilon_x^R \tag{18}$$

When additional data become available, an averaged ε_x^U estimation from all the data can be used to reduce the estimation error of the true ε_x^U.

3. Experimental validation using steel hollow cylinder in laboratory

3.1. Experimental setup

A hollow steel cylinder, made of SS400 steel alloy, was fabricated with an outer diameter of 13 mm and an inner diameter of 5 mm. The geometries and dimensions of the specimen are presented in Fig. 2 (a). Two 16 mm × 16 mm MFC transducers of the M0714-P2 type, manufactured by the Smart Material Corporation, were installed on the surface of the specimen to generate and obtain the L(0,1) mode. To obtain the reference (ground truth) absolute strain, reference unknown strain, and relative strain, a resistance-type strain gauge (FLA-1–11-1LJC) manufactured by Techni Measure was used. The specimen was subjected to various tensile force using an Instron 8801 hydraulic loading machine, as depicted in Fig. 2 (b).

For data acquisition, a National Instruments (NI) system was used consisting of an arbitrary waveform generator (AWG, NI PXI-5421) with 14-bit resolution, a two-channel digitizer (DIG, NI PXIe-5160) with 10-bit resolution, and a control unit (NI PXIe-8840), as depicted in Fig. 3. The AWG produced an ultrasonic input signal (three-cycle tone burst) while the DIG recorded the corresponding ultrasonic response, as shown in Fig. 3. The duration of the ultrasonic response was 2 ms and the sampling frequency of the DIG was 2.5 GHz. The frequency of the ultrasonic input signal was set to 15 kHz, taking into account that the L (0,1) mode velocity converged to the bar velocity. To improve the signal-to-noise ratio, the ultrasonic response were obtained 100 times and averaged in the time domain. The reference absolute strain, reference unknown strain, and relative strain were obtained using a strain input module (NI-9237) with a sampling rate of 100 kHz.

3.2. Validation of linear relationship derived between L(0,1) mode velocity and absolute strain

The derived linear relationship between the L(0,1) mode velocity (c_x^s) and absolute strain (ε_x) was validated using the data obtained from
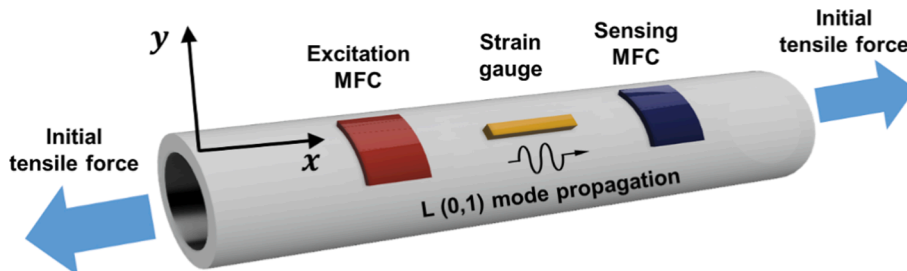

Fig. 1. Schematic of the sensors installed to obtain the L(0,1) mode and the relative strain.

(a)   (b)
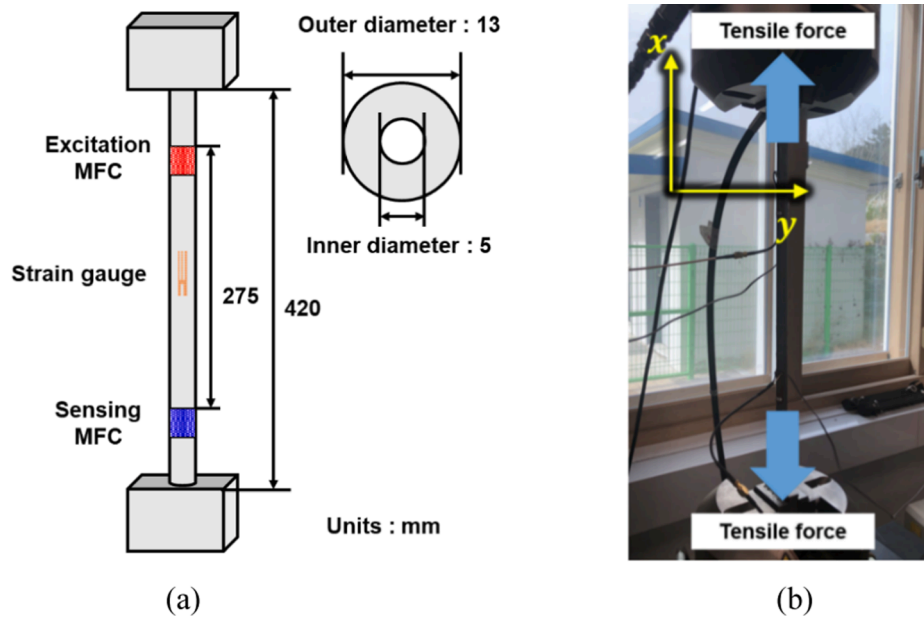
Fig. 2. Experimental setup for experimental validation using the hollow cylinder specimen in laboratory: (a) geometry and dimensions of the specimen, and (b) specimen installed in hydraulic loading machine (Instron 8801).
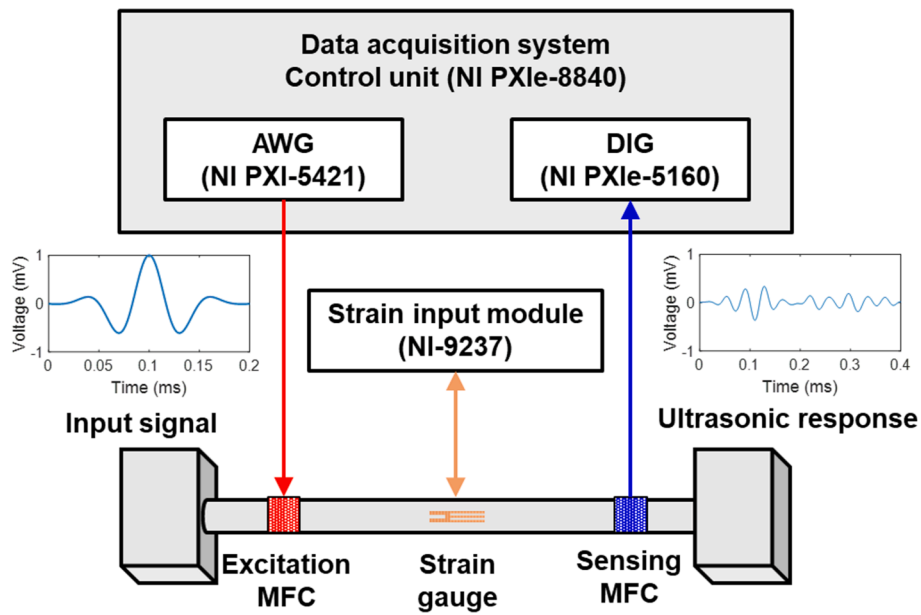

Fig. 3. Data acquisition system for absolute strain estimation.

(a)   (b)
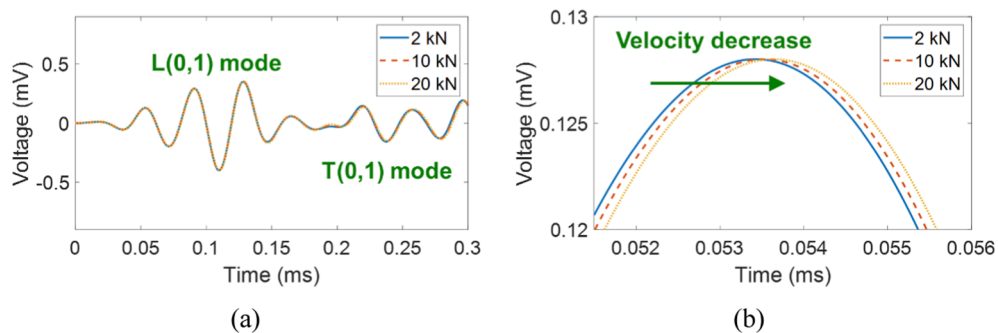
Fig. 4. Representative ultrasonic responses: (a) variation of L(0,1) and T(0,1) modes under varying tensile load, and (b) close-up of L(0,1) mode in (a).

the hollow cylinder specimen. The specimen was subjected to various tensile force levels in the *x*-direction, the ultrasonic responses are measured at each tensile force levels. Representative ultrasonic responses obtained from 2, 10, and 20 kN tensile force levels are shown in Fig. 4. Both L(0,1) and T(0,1) modes are clearly present in Fig. 4 (a). Fig. 4 (b) enlarges the L(0,1) mode wave packet and shows the decrease of c_x^s as the tensile force increases. The resulting c_x^s values according to the ε_x variation were obtained, as shown in Fig. 5. ε_x was obtained using the strain gauge installed when the tensile force is zero. The experimental values of the linear function between c_x^s and ε_x was obtained using linear regression analysis. The result of the linear regression analysis was quantitatively evaluated using the R^2 value, indicating a strong linearity ($R^2 = 0.9942$). The theoretical values of the linear function between c_x^s and ε_x in the hollow cylinder specimen, with the elastic modulus of 206 GPa, density of 7.85 g/cm^3, and Poisson's ratio of 0.3, were calculated using Eqs. (1) and (12), respectively. The experimental and theoretical values of the linear functions are listed in Table 1, which shows excellent agreement between the experimental and theoretical values. Therefore, a linear relationship between the L(0,1) mode velocity and absolute strain was successfully derived.

3.3. Baseline-free absolute strain estimation results

The performance of the developed absolute estimation technique was evaluated under two different tensile force cases. In the first case, tensile forces ranging from 2 kN to 20 kN were applied to the hollow cylinder specimen in 2 kN increments. Conversely, in the second case, the tensile force was varied from 20 to 2 kN in increments of 2 kN. In the first and second cases, the MFC transducers and strain gauges were installed on the specimens at 2 and 20 kN, respectively. First, c_{xU}^s was measured at ε_x^U induced by the initial tensile force (2 kN in the first case and 20 kN in the second case). Then, whenever the tensile force changed, c_{xR}^s and ε_x^R measurements were performed ten times at each tensile force level. Subsequently, the ε_x^U value was estimated using Eqations (17). Finally, ε_x was estimated by adding the estimated ε_x^U to the ε_x^R obtained using the strain gauge. The reference absolute strain and reference unknown strain were obtained by measuring the data using a strain gauge installed at a tensile force of 0 kN. For a quantitative performance evaluation, the maximum error (max. err) and normalized root-mean-square error (NRMSE) values were computed using the following expressions:

$$\text{Max. err} = max(|s_k - \widehat{s}_k|), \quad k = 1, 2, \cdots, n \tag{19}$$

and

$$\text{NRMSE (\%)} = \frac{\sqrt{\frac{1}{n}\sum_{k=1}^{n}(s_k - \widehat{s}_k)^2}}{\overline{s}} \times 100 \tag{20}$$

where s_k and $\widehat{s}_k$ are the reference absolute strains obtained by the strain gauge and the absolute strain estimated by the developed technique at
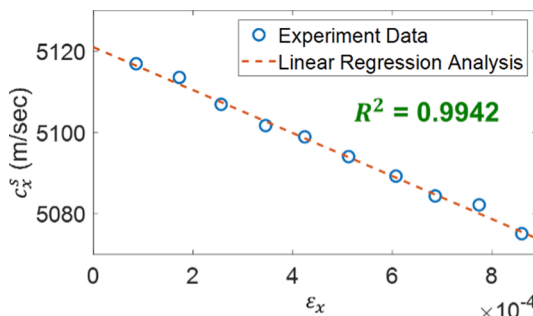

Fig. 5. Linear regression analysis between c_x^s and ε_x.

Table 1
Experimental and theoretical values of the linear function between c_x^s and ε_x.

	Experimental value	Theoretical value	Relative error[***]
Slope (*a*)[*]	52899.9	52766.9	0.25 %
y intercept (*b*)[**]	5121	5123	0.04 %

[*]*a* in the linear function $c_x^s = a\varepsilon_x + b$.

[**]*b* in the linear function $c_x^s = a\varepsilon_x + b$.

[***] Relative error = (|Theoretical value − Experimental value|)*100/Theoretical value.

the k-th measurement, respectively, and $\overline{s}$ denotes the mean of s_k.

The developed absolute strain estimation technique was applied to additional two hollow steel cylinder specimens. Figs. 6 and 7 demonstrate that the absolute error of the unknown strain decreases as more data is used for the unknown strain (ε_x^U) estimation, as discussed in Section 2.2. The absolute error is obtained by calculating the absolute value of the difference between the reference and estimated unknown strains. Equation (17) is derived assuming linear elastic behavior of the specimen material. However, because the initial tensile force of the second case is 20 kN, which is near the yield strength of the specimen (27.7 kN), the plasticity comes to play and the accuracy of Equation (17) deteriorates in the second case. So, the absolute strain estimation error of the second case was larger than the first case. The average values of Max. err and NRMSE for absolute strain estimation were 4.90e-5 and 4.04%, respectively. These findings indicate that the developed technique can effectively estimate the absolute strain. Notably, unlike the conventional absolute strain estimation technique, the developed technique can successfully estimate the absolute strain without calibration test and baseline data obtained from a known absolute strain levels.

4. Experimental validation using submerged floating tunnel in ocean engineering basin

4.1. Experimental setup

To evaluate the applicability of the developed technique in the field, a baseline-free absolute strain estimation was performed using an 8-meter-long SFT model. The SFT model comprised eight bolt-connected tubes, eight mooring cables, and a steel frame, as depicted in Fig. 8 (a). Each tube was one meter long and had a uniform cross-section with an outer diameter of 14 cm and an inner diameter of 13 cm. The mooring cables were made of aluminum 6061-T6 alloy and had an outer diameter of 13 mm and an inner diameter of 6 mm. One end of each mooring cable was connected to the tube, and the other end was connected to the steel frame using metal ring buckles. The steel frame was fixed to the ground using anchor bolts. The SFT model was submerged in an ocean engineering basin measuring 12 m long, 10 m wide, and 2 m deep, as illustrated in Fig. 8 (b).

Absolute strain estimation was performed for mooring cables 1, 2, 3, and 4 out of eight mooring cables, as shown in Fig. 8 (a). To obtain the L (0,1) mode and relative strain, two MFC transducers and one strain gauge were installed on the surfaces of the four mooring cables, as depicted in Fig. 8 (c). The data acquisition parameters such as the sensor type, frequency of the ultrasonic input signal, duration of the obtained ultrasonic response, and sampling frequency were the same as those in Section 3.1. To prevent failure, the sensors were waterproofed using a DOW CORNING RTV-3145. After waterproofing, water was poured into the ocean engineering basin to ensure that the SFT model was immersed and floating.

4.2. Baseline-free absolute strain estimation results

The MFC transducers and strain guage were assumed to be installed on the specimen at water level 0, as shown Fig. 9 (a). The L(0,1) mode
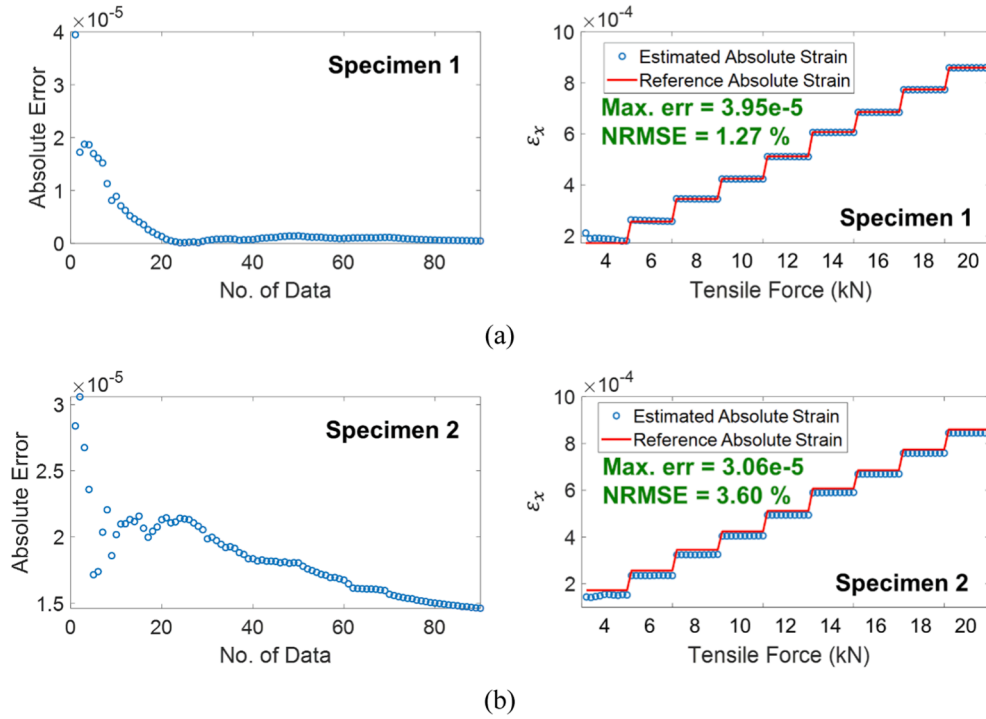
Fig. 6. Unknown strain and absolute strain estimation results for the first case (increasing tensile force): (a) specimen 1, and (b) specimen 2.
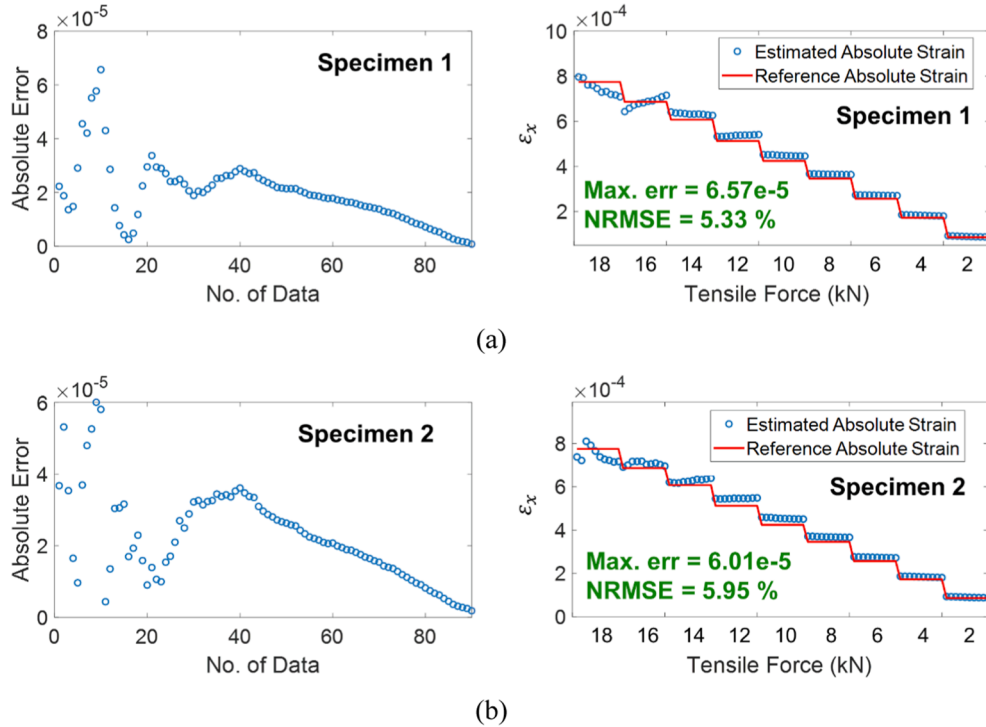

Fig. 7. Unknown strain and absolute strain estimation results for the second case (decreasing tensile force): (a) specimen 1, and (b) specimen 2.

and relative strain were measured at each water levels. The absolute strain variation induced by buoyancy and wave loading was estimated using only the L(0,1) mode and relative strain obtained after the sensors were installed. The reference absolute strain was obtained by measuring the data using a strain gauge before pouring water into the ocean engineering basin. Representative ultrasonic responses measured from mooring cable 1 under 0 and 4 water levels are shown in Fig. 9 (b) and

(c). Fig. 9 (c) enlarges the L(0,1) mode wave packet and shows the decrease of c_x^s as the water level increases similar to Fig. 4.
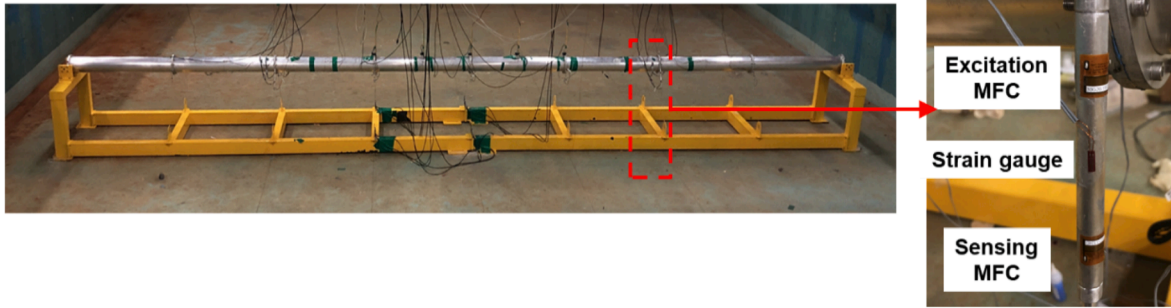
To investigate the accuracy of the absolute strain estimation, the max. err and NRMSE values were used, similar to the previous validation tests described in Section 3.3. The estimation results for the absolute strain variation induced by buoyancy are shown in Fig. 10 (a), (b), (c), and (d). The developed technique estimated the absolute strain with a
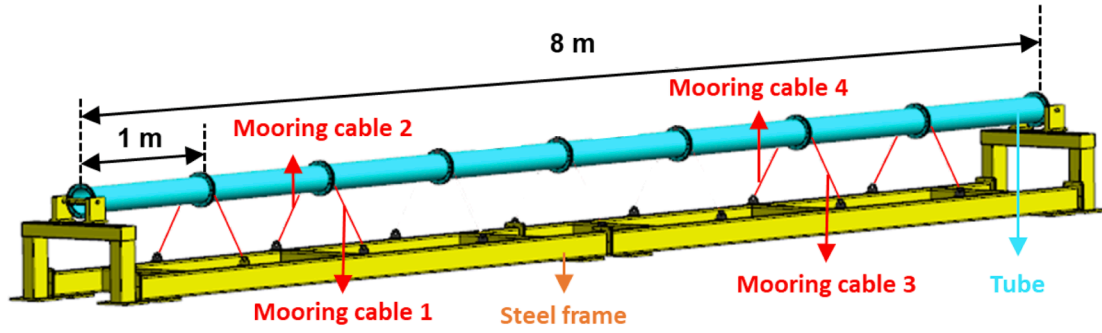
(a)
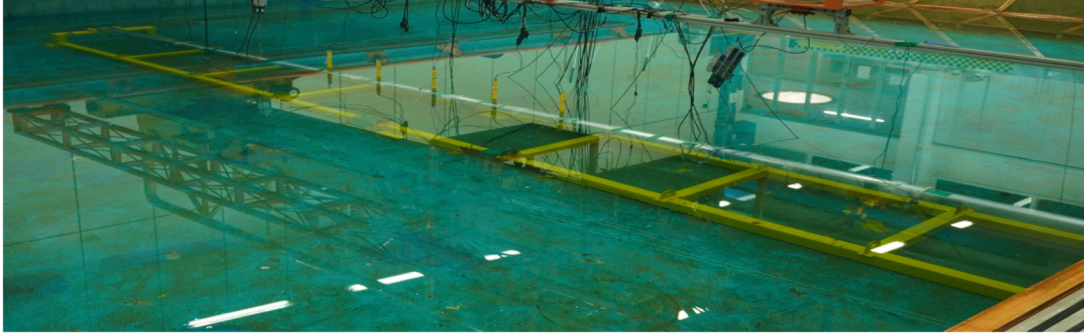
(b)

(c)

Fig. 8. Configuration of the 8-m-long SFT model: (a) geometry and dimensions of SFT model, (b) SFT model submerged into ocean engineering basin, and (c) installation of MFC transducers and strain gauge.

max. err of 1.30e-6 and an NRMSE of 3.95%.

The developed technique was used to estimate the absolute strain variation induced by wave loading after the SFT model was fully submerged in water. The wave loading applied to the SFT model had an angular frequency of 1.5 rad/s and an amplitude of 170 mm. The L(0,1) mode and relative strain were obtained eight times for mooring cables 1, 2, 3, and 4 when wave loading was applied to the SFT model. The absolute strain estimation was performed using the L(0,1) mode velocity and relative strain. The estimation results of the absolute strain variation induced by wave loading are shown in Fig. 11. The developed technique estimated the absolute strain within a max. err of 2.05e-6 and a NRMSE of 5.60%. The developed technique's field applicability is excellent, indicating its usefulness for in-service cylindrical structures where the MFC transducers and strain gauge were not initially installed before applying tensile force.

5. Conclusion

In this study, a baseline-free technique for estimating absolute strain of in-service cylindrical structures was developed based on the acoustoelastic effect of ultrasonic guided wave. The linear relationship between ultrasonic guided wave velocity and absolute strain was derived and experimentally verified on a steel hollow cylinder. To obtain the ultrasonic guided wave and relative strain, two MFC transducers and one strain gauge were installed on the surfaces of the cylindrical structures subjected to an initial tensile force. The unknown absolute strain was then estimated using the measured ultrasonic guided wave velocity and relative strain. To experimentally validate the performance of the developed technique, blind data was obtained from a steel hollow cylinder under two tensile force cases. The absolute strain estimation resulted in an average Max. err of 4.90e-5 and an average NRMSE of 4.04%. Unlike conventional absolute strain estimation techniques, the

(a)

(b)

(c)
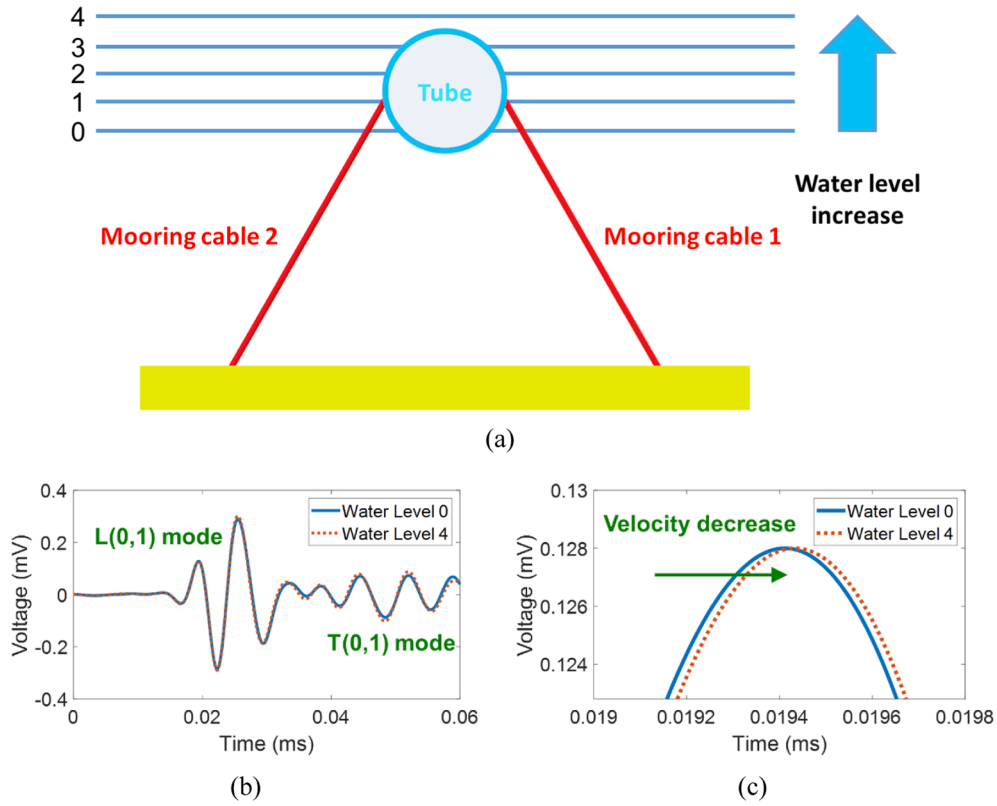
Fig. 9. Measurement of L(0,1) mode and relative strain under varying water levels: (a) water level variation, (b) representative ultrasonic responses measured from mooring cable 1 at 0 and 4 water levels, and (c) close-up of L(0,1) mode in (b).

(a)

(b)

(c)

(d)
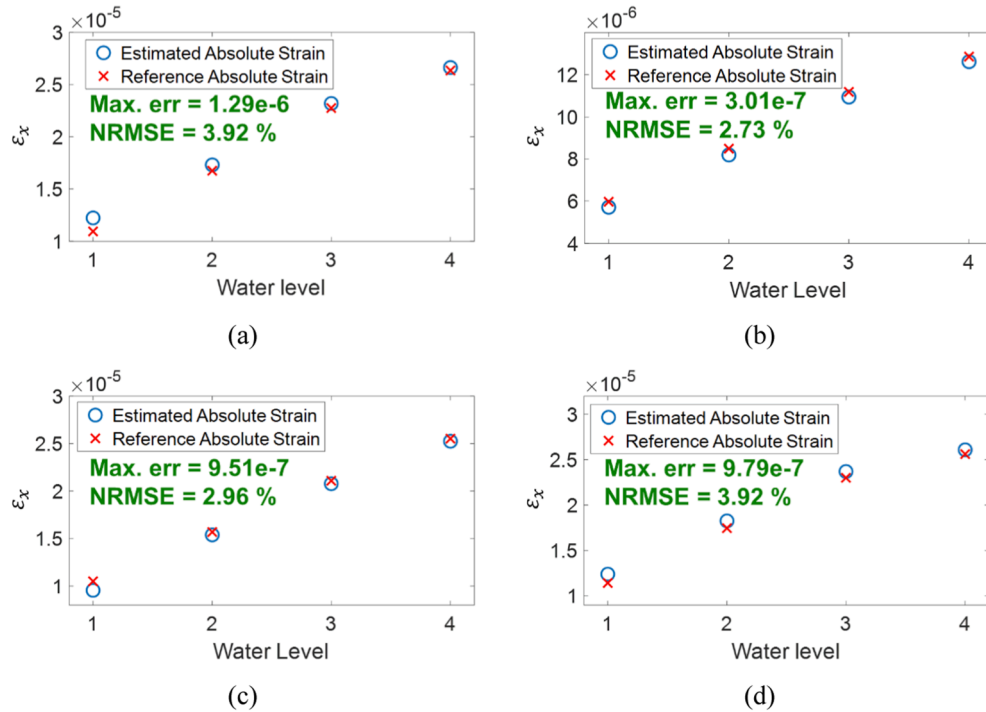
Fig. 10. Estimation results of absolute strain variation induced by buoyancy: absolute strain estimation for mooring cable (a) 1, (b) 2, (c) 3, and (d) 4.

developed technique estimates the absolute strain using only the data obtained after installing the sensors, without the need for calibration tests or baseline data.

To evaluate the applicability of the developed technique in the field,

baseline-free absolute strain estimation was performed for the mooring cables of a submerged floating tunnel (SFT) model in an ocean engineering basin. By estimating the absolute strain variation due to buoyancy and wave loading, the average Max. err was 1.30e-6 with an
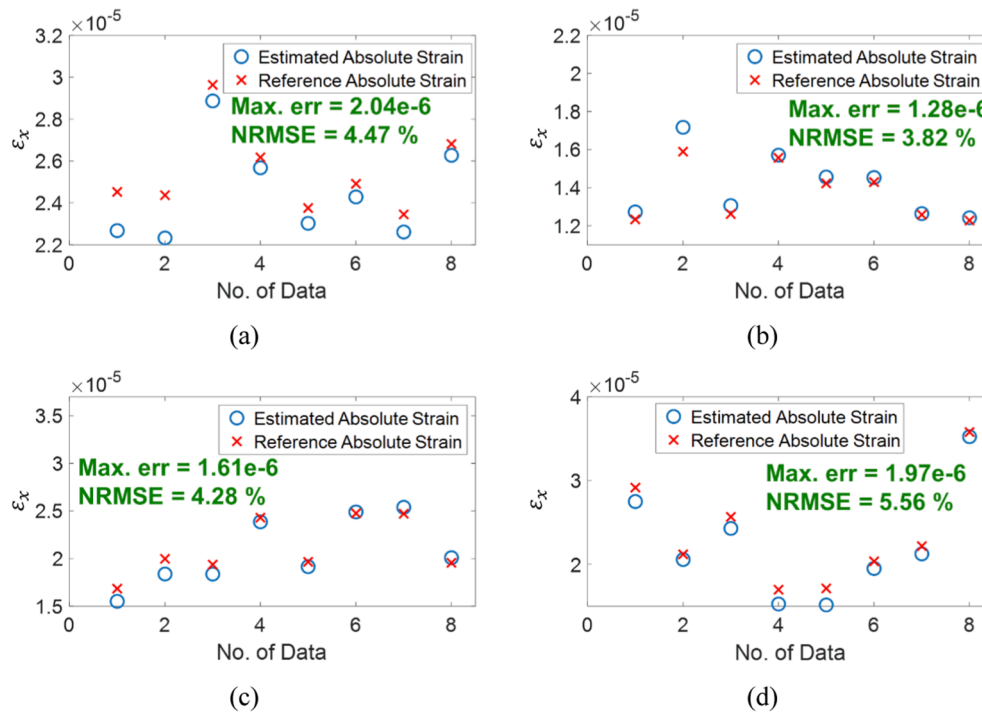
Fig. 11. Estimation results of absolute strain variation induced by wave loading: absolute strain estimation for mooring cable (a) 1, (b) 2, (c) 3, and (d) 4.

average NRMSE of 3.96%. Thus, the experimental results indicate that the developed technique can be applied to in-service cylindrical structures. The developed technique offers several unique features: (1) the linear relationship between ultrasonic guided wave velocity and absolute strain is newly derived and experimentally verified; (2) the absolute strain is estimated without the need for calibration tests and baseline data; (3) the developed technique is experimentally validated in laboratory and ocean engineering basin; and (4) the developed technique is applicable to in-service cylindrical structures where the MFC transducers and the strain gauge are not initially installed before applying force.

The developed baseline-free absolute strain estimation technique shows promise for in-service cylindrical structures. However, several issues must be addressed prior to actual field application. First, the ultrasonic guided wave velocity is not only affected by absolute strain but also by temperature. Therefore, it is necessary to compensate for the effect of temperature during absolute strain estimation. Second, the relationship between ultrasonic guided wave velocity and absolute strain was derived only for tensile forces, without considering biaxial and more complex force conditions. Future work is required to address these limitations and make the developed technique better suited for in-service cylindrical structures.

CRediT authorship contribution statement

Ohjun Kwon: Conceptualization, Methodology, Formal analysis, Validation, Writing – original draft. **Hoon Sohn:** Supervision, Writing – review & editing, Funding acquisition. **Jinho Jang:** Validation. **Jaemook Choi:** Validation. **Zhanxiong Ma:** Validation. **Hyung Jin Lim:** Writing – review & editing.

Declaration of Competing Interest

The authors declare that they have no known competing financial interests or personal relationships that could have appeared to influence the work reported in this paper.

Data availability

Data will be made available on request.

References

[1] Kwon O, Sohn H, Lim HJ. Ultrasonic-based tensile force estimation for cylindrical rod at various temperature conditions. Eng Struct 2022;265:114509. https://doi.org/10.1016/j.engstruct.2022.114509.

[2] Dębska A, Gwoździewicz P, Seruga A, Balandraud X, Destrebecq JF. The longitudinal compression capacity of hollow concrete cylinders prestressed by means of an SMA wire. Materials (Basel) 2022;15:826. https://doi.org/10.3390/ma15030826.

[3] Ni YQ, Chen R. Strain monitoring based bridge reliability assessment using parametric Bayesian mixture model. Eng Struct 2021;226:111406. https://doi.org/10.1016/j.engstruct.2020.111406.

[4] Kerrouche A, Boyle WJO, Sun T, Grattan KTV, Schmidt JW, Täljsten B. Enhanced FBG sensor-based system performance assessment for monitoring strain along a prestressed CFRP rod in structural monitoring. Sens Actuators A 2009;151:127–32. https://doi.org/10.1016/j.sna.2009.02.030.

[5] Du Y, Gou Z-M. Application of the non-contact video gauge on the mechanical properties test for steel cable at elevated temperature. Appl Sci 2019;9:1670. https://doi.org/10.3390/app9081670.

[6] Gulgec NS, Takáč M, Pakzad SN. Structural sensing with deep learning: Strain estimation from acceleration data for fatigue assessment. Comput Aid Civ Infrastruct Eng 2020;35:1349–64. https://doi.org/10.1111/mice.12565.

[7] Yi X, Cho C, Cooper J, Wang Y, Tentzeris MM, Leon RT. Passive wireless antenna sensor for strain and crack sensing—Electromagnetic modeling, simulation, and testing. Smart Mater. Struct. 2013;22:085009. https://doi.org/10.1088/0964-1726/22/8/085009.

[8] Zhou K, Wu ZY. Strain gauge placement optimization for structural performance assessment. Eng Struct 2017;141:184–97. https://doi.org/10.1016/j.engstruct.2017.03.031.

[9] Toyama N, Takatsubo J. An investigation of non-linear elastic behavior of CFRP laminates and strain measurement using Lamb waves. Compos Sci Technol 2004;64:2509–16. https://doi.org/10.1016/j.compscitech.2004.05.007.

[10] Gandhi N, Michaels JE, Lee SJ. Sang Jun Lee, Acoustoelastic Lamb wave propagation in biaxially stressed plates. J Acoust Soc Am 2012;132(3):1284–93.

[11] Dodson JC, Inman DJ. Investigating the thermally induced acoustoelastic effect in isotropic media with Lamb waves. J Acoust Soc Am 2014;136(5):2532–43. https://doi.org/10.1121/1.4897310.

[12] Li ZH, Wang YZ, Zheng JC, Liu NX, Li M, Teng J. Stress measurement for steel slender waveguides based on the nonlinear relation between guided wave group velocity and stress. Measurement 2021;179:109465. https://doi.org/10.1016/j.measurement.2021.109465.

[13] Nishino H, Takashina S, Uchida F, Takemoto M, Ono K. Modal Analysis of Hollow Cylindrical Guided Waves and Applications. Jpn J Appl Phys 2001;40(1R):364.

[14] Chai HY, Phoon KK, Zhang DJ. Effects of the source on wave propagation in pile integrity testing. J Geotech Geoenviron Eng 2010;136:1200–8. https://doi.org/10.1061/(ASCE)GT.1943-5606.0000272.

[15] Nishino H, Takemoto M, Chubachi N. Estimating the diameter/ thickness of a pipe using the primary wave velocity of a hollow cylindrical guided wave. Appl Phys Lett 2004;85(6):1077–9. https://doi.org/10.1063/1.1781353.

[16] Seco F, Martín JM, Jiménez A, Pons JL, Calderón L, Ceres R. PCDISP: A tool for the simulation of wave propagation in cylindrical waveguides. In: 9th International Congress on Sound and Vibration 2002.

[17] Courtney TH. Mechanical Behavior of Materials. Waveland Press; 2005.

[18] Wood WW, Parker FR. Monte Carlo equation of state of molecules interacting with the Lennard-Jones potential I. A supercritical isotherm at about twice the critical temperature. J Chem Phys 1957;27:720–33. https://doi.org/10.1063/1.1743822.

[19] Kumar N, Juneja JK. Comprehensive objective physics. Bells: Golden; 2006.

[20] Yu X, Zuo P, Xiao J, Fan Z. Detection of damage in welded joints using high order feature guided ultrasonic waves. Mech Syst Signal Process 2019;126:176–92. https://doi.org/10.1016/j.ymssp.2019.02.026.